Characterization and quantification of the interaction between the NFL-TBS.40-63 peptide and lipid nanocapsules

A. Griveau [a], H. Alnemeh-Al Ali [a], M.A. Jourdain [a], A. Dupont [b], J. Eyer [a,*]

[a] *Univ Angers, Inserm, CNRS, MINT, SFR ICAT, F-49000 Angers, France*
[b] *Univ Rennes, CNRS, Inserm, BIOSIT-UMS 3480, US_S 018, Rennes, France*

ARTICLE INFO

ABSTRACT

Several studies previously showed that the NFL-TBS.40–63 peptide (NFL-peptide) is capable to specifically penetrating several glioblastoma cell lines (rat, mouse, human) and inhibiting their cell division *in vitro* and their tumor development *in vivo*. When lipid nanocapsules (LNCs) are functionalized with the NFL-peptide, their absorption is targeted in glioblastoma cells both *in vitro* and *in vivo*. In the present study, we investigated the molecular architecture of these nanovectors (LNC-NFL) by using several microscopy techniques (transmission electron microscopy, cryo-electron microscopy, and cryo-electron tomography). We also used high-performance liquid chromatography (UPLC) technique to evaluate the interaction between LNCs and peptides. The work shows that the NFL-peptide forms stable long filaments along which the lipid nanocapsules interact strongly to form some sort of nanomolecular bracelets. This new construction composed of the NFL-peptide and lipid nanocapsules shows a better internalization in rat glioblastoma cells (F98 cells) than lipid nanocapsules alone.

1. Introduction

The discovery of nanoparticles offers new opportunities for the development of biomedical technologies. The main goal of such nanoparticles is to improve the efficiency of therapeutic molecules including a targeted accumulation of the drug, its protection from degradation, and the reduction of its side effects (Suri et al., 2007). Moreover, the nanometric size of such nano-vehicles allows a better crossing of biological barriers, but also induces toxicity when they do not target specific cells (Barry and Vertegel, 2013). Nanoparticles can be used to improve the pharmacological and therapeutical properties of drugs, proteins, or peptides. Finally, the different types of conjugation between nanoparticles and encapsulated molecules protect these compounds against degradation, increase their presence in the body and reduce their toxicity (Pudlarz and Szemraj, 2018). Many types of nanoparticles of different shapes and compositions can be produced and used (Shapira

et al., 2011). For example, micelles (Malmsten and Lindman, 1992), lipid nanoparticles: such as liposomes (Schnyder et al., 2005), lipid nanocapsules (Heurtault et al., 2002), solid nanoparticles (Lazăr et al., 2019), polymeric nanoparticles (Kreuter, 2004) or metallic nanoparticles (Zhu et al., 2017) were developed. In our laboratory we produced since several years lipid nanocapsules (LNCs), which are composed of a liquid oily heart made up of triglycerides surrounded by non-ionic phospholipid surfactants and amphiphilic polymers constituting a solid shell. These excipients are biocompatible, Food and Drug Administration approved and formulated using a process phase inversion not requiring solvents (Heurtault et al., 2002). Depending on the proportion of excipients used, the size of LNCs may vary from 20 nm to 100 nm, with a rather monodisperse distribution and a very good stability (Heurtault et al., 2003). While the size of these nano-objects can be well controlled and represents a major advantage for crossing certain biological barriers, a major challenge is to target the entry of such

---

objects into specific tissues or cells, like in cancer cells and not in healthy cells.

Peptides represent another important part of such nanosystems, and they have been mainly used as therapeutic molecules or for improved targeting. The first peptide used in combination with nanoparticles to improve its delivery throughout the body is the TAT cell-penetrating peptide (CPP) derived from the human immunodeficiency virus (HIV) (Vivès et al., 1997; Schwarze, 1999). This peptide was then coupled to different nano-vehicles such as micelles, liposomes, chitosan nanoparticles or silver nanoparticles (Qin et al., 2012; Rudolph et al., 2004). Several studies have shown interesting results of nanoparticles coupled with CPP for the treatment of cancers (Jiang et al., 2012; Wei et al., 2018). A study has shown that the use of poly(ethylene glycol)-poly (ε-caprolactone) copolymers (PEG-PCL) nanoparticles functionalized with a cell-penetrating peptide (Angiopep-2) and containing an anticancer agent (Paclitaxel) promotes the specific apoptosis of glioma cells and accumulation *in vivo* in the tumor (Xin et al., 2011). Another study using the same CPP, nanoparticles and Docetaxel, showed an important antitumor effect on glioblastoma (GBM) with an increase of mice survival (Gao et al., 2014).

For several years, we have been studying a peptide called NFL-TBS.40–63 (or NFL-peptide), which has the interesting property of targeting and penetrating GBM cells (human, mouse, and rat) *in vitro*, and glioma tumors *in vivo*. Another amazing activity of this peptide is to interact with the free tubulin present in these cells and to inhibit its polymerization into microtubules, thus affecting their proliferation and inducing their apoptosis (Berges et al., 2012). This peptide can be coupled to LNCs filled with an anticancer drug (Paclitaxel), to target and enhance LNCs internalization *in vitro* in mouse GBM cells, and *in vivo* in brain implanted GBM tumors in mice. These NFL-peptide functionalized LNCs loaded with Paclitaxel reduce tumor volume by 75–80%, whereas LNCs loaded only with Paclitaxel and without the NFL-peptide reduce tumor volume by only 50–60% (Balzeau et al., 2013).

In this study, we showed that when the NFL-peptide is biotinylated, it can assemble into long nanofilaments and can strongly bind LNCs by concentrating them into some sort of nano-bracelets, which can massively enter GBM cells. On the contrary, when the NFL-peptide is coupled to 5-carboxyfluorescein (FAM-NFL), it cannot form such filaments, but it can interact with LNCs and can also increase their entry into GBM cells. The nude-NFL-peptide (without Biotin, or FAM) forms small fibrils but not filaments. Finally, the NFL-SCR-peptides, which consist of the same amino-acids but in a scrambled order, show an extremely poor ability to enter rat GBM cells with Biotin, or FAM, although they form filaments. Together, these results demonstrate a new way to elaborate nanovectors based on the unique properties of this NFL-peptide. In this paper, different techniques and methodologies were used to characterize and quantify the interaction between the NFL-peptide, lipid nanocapsules, and GBM cells. We will discuss the contributions of these techniques, but also their limits. Indeed, several of these techniques are commonly used in the world of nanotechnology, but our work shows that some of them must be used with great caution to avoid misinterpretations.

2. Material and methods

2.1. Reagents

The NFL-TBS.40–63 peptide (NH$_2$-YSSYSAPVSSSLSVRRSYSSSSGS-CONH$_2$) was synthesized by PolyPeptide Group (Strasbourg, France), and it can be nude (nude-NFL-peptide), biotinylated (BIOT-NFL-peptide), or coupled to 5-carboxyfluorescein (FAM-NFL-peptide). Addition of the fluorophore (BIOT, or FAM) to the NFL-peptide was achieved by an amide bond. Concerning the nude-NFL-peptide, it was synthetized by PolyPeptide Group or by ourselves to determine eventual differences of activities. Two scrambled peptides synthetized by Millegen (Toulouse, France) were used: BIOT-NFL-SCR (BIOT-SPSVSYSRSGSYSASRSLSYSVSS-CONH$_2$) and FAM-NFL-SCR (FAM-SLGSPSSSVRASYSSSRSYVYSSS-CONH$_2$).

All amino acids, diisopropylethylamine (DIEA), piperidine and 2-(1H-benzotriazol-1-yl)-1,1,3,3-tetramethyluronium hexafluorophosphate (HBTU) were obtained from Iris Biotech GmbH (Marktredwitz, Germany). Rink amid *p*-methylbenzhydrylamine (MBHA) resin was purchased from Multisyntech GmbH (Witten, Germany). Methyl alcohol (MeOH), trifluoroacetic acid (TFA), dimethylformamide (DMF) and thioanisole triisopropyl silane were used for the synthesis from Thermo Fisher Scientific (Massachusetts, USA). Deionized water was recovered from a MilliQ plus system from Merck-Millipore (Darmstadt, Germany). Phenol was purchased from Merck KGaA (Germany). Diethyl ether, and LC-MS water grade were obtained from Biosolve (Dieuze, France). Acetonitrile and formic acid were from Sigma-Aldrich (Saint-Quentin-Fallavier, France).

2.2. Peptide preparation

The peptides (BIOT-NFL, BIOT-NFL-SCR, FAM-NFL, FAM-NFL-SCR, or nude-NFL) were dissolved in sterile water at the concentration of 1 mmol/L. Electron microscopic observations of all samples were performed to assess the ability of the NFL-peptide to self-assemble (or not) in water. These experiments were carried out in at least triplicate.

2.3. Transmission electron microscopy

Samples observations were performed with a transmission electronic microscope (TEM) in the Microscopy Rennes Imaging Center platform (MRic TEM, Rennes, France). Samples were deposited (4 μL) into carbon films on copper grids (300 mesh) for 1 min and negatively staining with 2% uranyl acetate for 10 s. Then, the samples were observed using a 200 kV Tecnai G^2 T20 Sphera, FEI microscope with a USC 4000 (Gatan) 4 k × 4 k CCD camera. Pictures were acquired using the camera in binning mode 1 and at a nominal magnification of 50,000 x, providing a pixel size of 0.22 nm.

2.4. The nude-NFL-peptide synthesis

The nude-NFL-peptide was synthesized according to the Fmoc solid phase peptide synthesis (SPPS) process already described by (Guyon et al., 2019) on a specific resin (0.52 mmol/g) using an automated microwave peptide synthesizer (Microwave Peptide Synthesizer, Liberty 1, CEM Corporation, Matthews, USA). Briefly, the resin was prepared in DMF, then two steps allowed to obtain the peptide chain: first the deprotection and secondly the accessibility of amino function. An appropriate cleavage solution was added to separate the nude-NFL-peptide from the resin and to remove the protective groups from the amino acid side chains (TFA/ phenol/water and TIS corresponding to a volume ratio of 88:5:5:2). After that, the nude-NFL-peptide was precipitated and followed by a centrifugation (2000 rpm, 30 min, 4 °C). Finally, the peptide was dissolved in a solution of H$_2$O/ACN (50/50; *v*/v) Waters, and the resulting sample was frozen and lyophilized.

2.5. Purification and characterization of the nude-NFL-peptide

To purify the peptide, semi preparative high-performance liquid chromatography (HPLC) from Waters instrument (Waters, Saint-Quentin-en-Yvelines, France) was carried out, according to the protocol previously published by Guyon et al., 2019. Specifically, to elute the nude-NFL-peptide a H$_2$O/ACN gradient was applied (90/10, *v*/v; Waters) (Supplemental Table S1). The peptide was prepared at 6 mg/mL in H$_2$O/ACN (60/40, v/v; Waters), and the chromatographic profile was obtained (Supplemental Fig. S1).

The nude-NFL-peptide was characterized by LC-MS/MS method using an Alliance® 2695 system (Waters). The same parameters were applied as previously described by Guyon et al., 2019. The column used was an Uptisphere C18 50 dB (Interchim, Montluçon, France).

Depending on the peptide analyzed, a H_2O/ACN specific gradient elution was applied (95/5, v/v; Waters; Supplemental Table S2), and the peptide was dissolved at 10 mg/mL in water/ACN. The m/z applied was 200–2000 range (full scan acquisition and the cone ramp 30 was used to detect the nude-NFL-peptide; Supplemental Fig. S2).

2.6. Preparation and characterization of lipid nanocapsules (LNC) labeled with DiD (LNC-(DiD)) and their functionalization with peptides

Lipid nanocapsules (50 nm) were prepared according to a previously described method (Heurtault et al., 2002). Typically, 0.846 g Kolliphor HS15 (BASF, Ludwigshafen, Germany), 1.028 g Labrafac WL 1349 (Gatefossé SA, Saint-Priest, France), 0.075 g Lipoïd S75–3 (Lipoïd Gmbh, Ludwigshafen, Germany), 0.089 g NaCl (Prolabo, Fontenay-sous-Bois, France) and 2.962 mL of water obtained from a MilliQ plus system (Millipore), were mixed and heated and cooled between 60 °C and 90 °C under magnetic stirring.

For LNC-(DiD), 27.5 μL of DiD solution (1,1′-dioctadecyl-3,3,3′,3′-tetramethylindodicarbocyanine, 4-chlorobenzenesulfonate, D7757; Thermo Fisher Scientific) at 1 mg/mL in absolute ethanol was added during the last cooling at 80 °C (the temperature of the phase inversion zone). To freeze the system, 12.5 mL of cold water was added.

Then, LNCs without or with the DiD probe were cooled under magnetic stirring for 5 min (Heurtault et al., 2002). The adsorption between peptides (BIOT-NFL, BIOT-NFL-SCR, FAM-NFL, FAM-NFL-SCR, or nude-NFL) and LNC-(DiD), was realized by an incubation between 369 μL of 1 mmol/L of peptide and 1 mL of 200 mg/mL of LNC or LNC-(DiD), overnight at room temperature under gentle stirring (Balzeau et al., 2013; Carradori et al., 2020, 2016). Experiments were performed at least in triplicate.

LNC-(DiD) with or without the peptide were characterized using a Malvern Zetasizer Nano Serie DTS 1060 (Malvern Instruments S.A., Worcestershire, UK) by hydrodynamic diameter, polydispersity index (PDI) and zeta potential measurements. LNCs were diluted 1/60 (*v*/*v*) in MilliQ purified water and the measurements were realized at 25 °C in triplicate.

2.7. Cryo-electron microscopy (CEM)

Analysis and observation of the NFL-peptide functionalized LNC samples were performed by cryo-electron microscopy on the Microscopy Rennes Imaging Center platform (MRic TEM, Rennes, France) to preserve the ultrastructural integrity of lipid nanocapsules. Vitrification of 50 nm-LNC-BIOT-NFL-peptide samples was performed using an automatic plunge freezer (EM GP, Leica) under controlled humidity and temperature (Dubochet and McDowall, 1981). Samples were deposited to glow-discharged electron microscope grids followed by blotting and vitrification by rapid freezing. Then, they were observed using a 200 kV electron microscope (Tecnai G^2 T20 Sphera, FEI) equipped with a 4 k × 4 k CCD camera (model USC 4000, Gatan). Micrographs were acquired under low electron doses using the camera in binning mode 1 and at a nominal magnification of 29,000 X. Observations were performed three times on independent experiments. In general, at least 50 images were taken per microscopy grid.

2.8. Cryo-electron tomography (Cryo-ET)

Analysis and observation by Cryo-Electron Tomography of the samples were also performed on the platform of the Microscopy Imaging Center Rennes (MRic TEM, Rennes, France) in order to follow at different levels, the continuity of the ultrastructural integrity of the filaments formed by the peptide and the fixation of LNC along these filaments. Vitrification of purified 50 nm-LNC-BIOT-NFL-peptide samples was performed using an automatic plunge freezer (EM GP, Leica) under controlled humidity and temperature (Dubochet and McDowall, 1981). Mix-capped gold nanoparticles of 10 nm in diameter (Duchesne et al.,

2008) were added to the sample at a final concentration of 80 nmol/L to be used as fiducial markers. Samples were deposited to glow-discharged electron microscope grids followed by blotting and vitrification by rapid freezing into liquid ethane. Grids were transferred to a single-axis cryoholder (model 626, Gatan) and were observed using a 200 kV electron microscope (Tecnai G^2 T20 Sphera, FEI) equipped with a 4 k × 4 k CCD camera (model USC 4000, Gatan). Single-axis tilt series, typically in the angular range ± 60°, were acquired under low electron doses (~0.3 e−/Å^2) using the camera in binning mode 2 and at a nominal magnification of 29,000 X. Images were taken every 5 slices, the distance between images is 3.9 nm and the voxel size is of 0.78768 nm. Tomograms were reconstructed using the graphical user interface eTomo from the IMOD software package (Mastronarde, 1997). Slices through the tomograms were extracted using the graphical user interface 3dmod of the IMOD package. Experiments were performed three times on independent samples.

2.9. Quantification of the interaction between peptide and LNC using the Size-Exclusion Chromatography/Ultra-Performance Liquid Chromatography system (SEC/UPLC)

This interaction was evaluated according a previously published protocol (Gazaille et al., 2021). We used an Acquity UPLC® Protein BEH SEC Guard Column (200 Å, 1.7 μm, 4.6 mm × 30 mm; Waters) and an Acquity UPLC® BEH 200 SEC Column (1.7 μm, 4.6 mm × 150 mm; Waters). Parameters used are a mobile phase of NaCl at 0.1 mol/L in water, a flow rate at 0.3 mL/min, a volume of injection of 10 μL and a detection wavelength of the UV detector of 220 nm. A calibration curve was determined for LNCs, for NFL-peptides (BIOT, FAM, or nude) and for scrambled peptides (BIOT, or FAM) by using different concentrations: between 5 and 300 μmol/L for peptides, and between 5 and 30 mg/mL for LNC concentrations. Then, the area under the peak was determined with Empower3 software (Waters). The peptide quantity interacting with LNC surface can be determined by separating free peptide from peptide-LNC.

2.10. Cellular uptake analysis of LNC-(DiD) functionalized or not with peptides by flow cytometry and confocal microscopy

Rat glioblastoma cells (F98) were cultured in Dulbecco's modified Eagle's medium (DMEM; Sigma-Aldrich) containing GlutaMax and supplemented with 10% of fetal bovine serum (Sigma-Aldrich), 1% of antibiotics (100× streptomycin/penicillin; BioWest, Nuaille, France) and 1% of non-essential amino acids (Sigma-Aldrich). F98 cells were seeded in 6-well plates at 400,000 cells per well and were incubated for 24 h at 37 °C and 5% CO_2. Then, LNC-(DiD) without or with the peptides (BIOT-NFL, BIOT-NFL-SCR, FAM-NFL, FAM-NFL-SCR, or nude-NFL) were incubated with cells at different concentrations (0.2, 0.5, 1 or 2 mg/mL of LNC-(DiD)) for 6 h. All experiments were also realized with the nude-NFL-peptide synthetized by PolyPeptide Group or synthetized in our laboratory. After incubation, cells were washed with 1× DPBS (Dulbecco's Phosphate Buffered Saline; Gibco, Dardilly, France) and with DMEM free, and the cells were incubated with 1× trypsin (Gibco) for 5 min. Then, F98 cells were centrifuged at 1200 rpm for 5 min, washed with 1× DPBS, diluted in 400 μL of 1× DPBS and counterstained with Propidium Iodide (50 μg/mL, P4867; Sigma-Aldrich) before analysis on a MACSQuant Analyzer (Miltenyi, Paris, France) and using the FlowJo Software (BD Biosciences, Paris, France). The analysis was realized and gated only live cells. Experiments were performed at least in triplicate, and 20,000 cells were measured for each experiment.

For confocal experiments, 25,000 F98 cells were seeded in 24-well plates coated coverslips for 48 h at 37 °C. Then, treatments of 6 h with LNC-(DiD) at 2 mg/mL, coupled or not with the different peptides were performed. This treatment time of 6 h is sufficient to assess the entry of LNCs with or without the peptides into living cells. All experiments were also realized with the nude-NFL-peptide synthetized by

PolyPeptide Group or synthetized in our laboratory. After incubation, cells were washed three times with $1\times$ DPBS, fixed with 4% para-formaldehyde (15,714; Delta microscopies, Mauressac, France) for 10 min, incubated with 0.2% X-100 triton (T9284; Sigma-Aldrich) diluted in $1\times$ DPBS for 15 min, then, with 5% bovine serum albumin (BSA, A7030; Sigma-Aldrich) diluted in $1\times$ DPBS for 30 min. For peptides coupled with the Biotin, an incubation of 1 h at room temperature with Alexa Fluor™ 488 Streptavidin conjugate (S32354; Thermo Fisher Scientific) diluted in $1\times$ DPBS/5% BSA at 1:500 was performed. Then, for all conditions, cells were incubated with 4′6-diaminido-2-phenylindole (DAPI, D9542; Sigma-Aldrich) diluted at 1:300 in $1\times$ DPBS for 10 min. The mounting with coverslips was performed with the Prolong Gold Antifade reagent (P36930; Thermo Fisher Scientific). Observations of the cells were performed using a confocal microscope (Leica TCS SP8; Leica Biosystems, Nanterre, France). The wavelengths used are respectively: DAPI: 410–450 nm, FAM: 493–540 nm, and DiD: 638–700 nm.

2.11. Statistical analysis

All data are represented as mean $\pm$ SEM. All experiments are repeated at least three times. Statistical analyzes were performed with Student's test using GraphPad Prism 7.03 (GraphPad software, San Diego, USA). The asterisks indicate significant level *$p < 0.05$; **$p < 0.005$ and ***$p < 0.001$.

3. Results

3.1. The BIOT-NFL-peptide can self-assemble into nanofilaments

The NFL-peptides prepared in water were examined by transmission electron microscopy (TEM). Interestingly, TEM micrographs revealed that the BIOT-NFL-peptide can spontaneously self-assemble into nanofilaments in sterile water (Fig. 1A). Nanofilaments are about 5 nm diameter and several micrometers long. Surprisingly, the BIOT-NFL-SCR which is composed of the same amino acids as the BIOT-NFL-peptide but in a random order, also forms short nanofilaments, but with a different
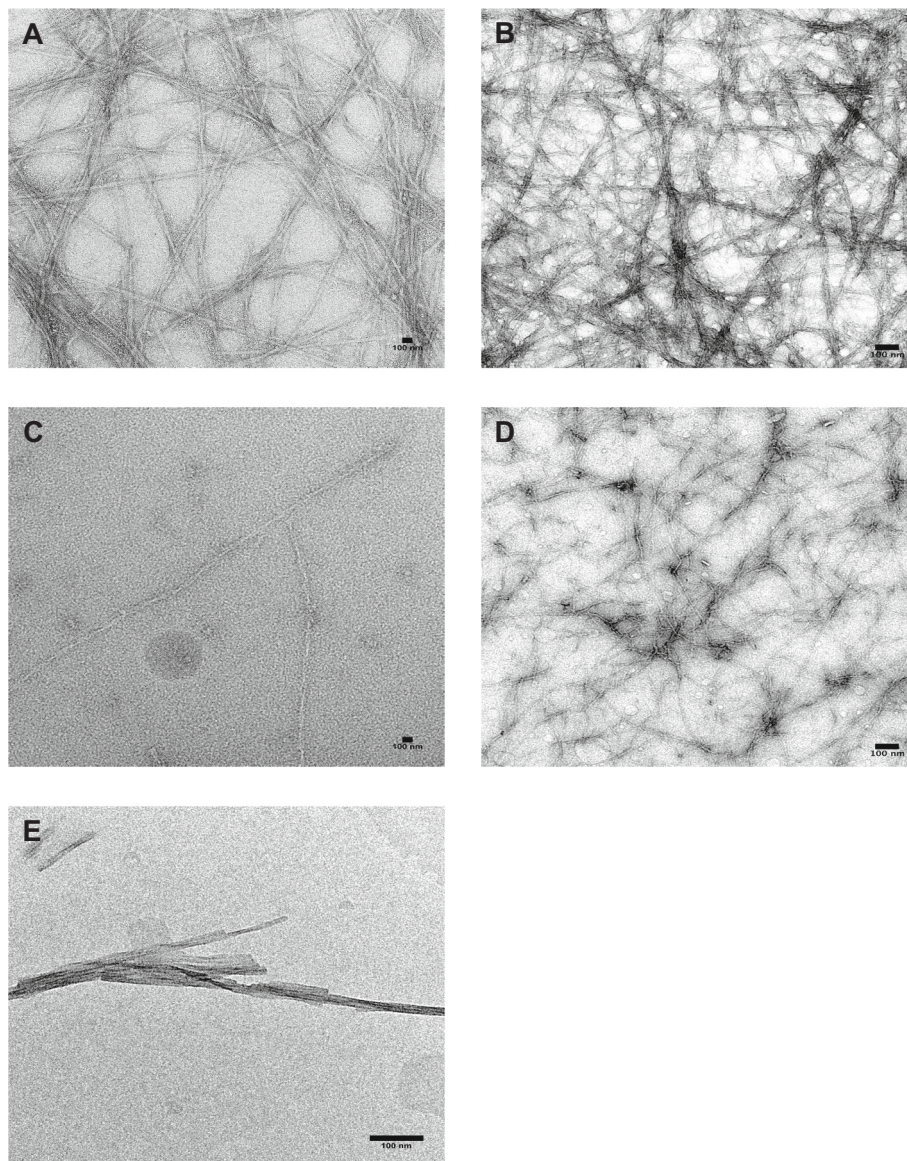
Fig. 1. Observations by transmission electron microscopy (TEM) of the self-assembly of the NFL-peptides (BIOT, FAM, or nude) and the scrambled peptides (BIOT, or FAM) diluted in sterile water at 1 mmol/L. (**A**) The BIOT-NFL, (**B**) the BIOT-NFL-SCR, (**C**) the FAM-NFL, (**D**) the FAM-NFL-SCR, (**E**) and the nude-NFL.. Scale bar: 100 nm. Experiments were performed at least in triplicate.

appearance (Fig. 1B). The FAM-NFL-peptide (Fig. 1C) very rarely forms short fibrils, and the FAM-NFL-SCR peptide forms a few very fine filaments (Fig. 1D). The formation of nanofilaments is not solely dependent on the presence of Biotin, as FAM-NFL-SCR formed short nanofilaments and not the FAM-NFL-peptide. For the nude-NFL-peptide (synthesized in two different ways), short and rigid fibrils were rarely observed but no filaments (Fig. 1E).

### 3.2. Lipid nanocapsules adsorb along BIOT-NFL-nanofilaments

We analyzed by cryo-electron microscopy (CEM) the molecular architecture of the nano-objects formed by LNCs functionalized or not with these different peptides. Cryo-electron microscopy best preserves the molecular architecture of lipid nanocapsules because it does not use dehydration or staining such as negative staining with uranyl acetate. Interestingly, micrographs showed that the BIOT-NFL-peptide is self-assembled into nanofilaments along which LNCs were adsorbed forming typical nano-bracelets. Interestingly, only very few free LNCs (not interacting with the filaments formed by the BIOT-NFL-peptide) were observed (Fig. 2A).

To further investigate the organization of these nano-bracelets, we performed cryo-electron tomography (cryo-ET) experiments on 50 nm-LNC-BIOT-NFL-peptide. This technique avoids possible artifact due to staining or drying of samples and confirms the 3D organization of LNCs and filaments. Using this approach, we confirm that LNCs interact with BIOT-NFL-peptide nanofilaments and that they are organized around these nanofilaments like some sort of nano-bracelets. Indeed, on each slice, we observed that most if not all LNCs are adsorbed along the filaments formed by the BIOT-NFL-peptide, and we can note the quasi absence of free LNCs (Fig. 2B). LNCs alone or incubated with the FAM-NFL-peptide do not show this ultra-structural organization (data not shown).

3.3. Quantification of the interaction between NFL-peptide and lipid nanocapsules: Size-Exclusion Chromatography/Ultra-Performance Liquid Chromatography system (SEC/UPLC) and cryo-electron microscopy (CEM)

To assess the amount of peptide interacted with the LNC surface, we used the Size-Exclusion Chromatography/Ultra-Performance Liquid-Chromatography (SEC/UPLC) method published by Gazaille et al., 2021. The first step was to inject different concentrations of LNCs (between 5 and 30 mg/mL) and different concentrations (between 5 and 300 μmol/L) of peptides (BIOT-NFL, BIOT-NFL-SCR, FAM-NFL, FAM-

A

B
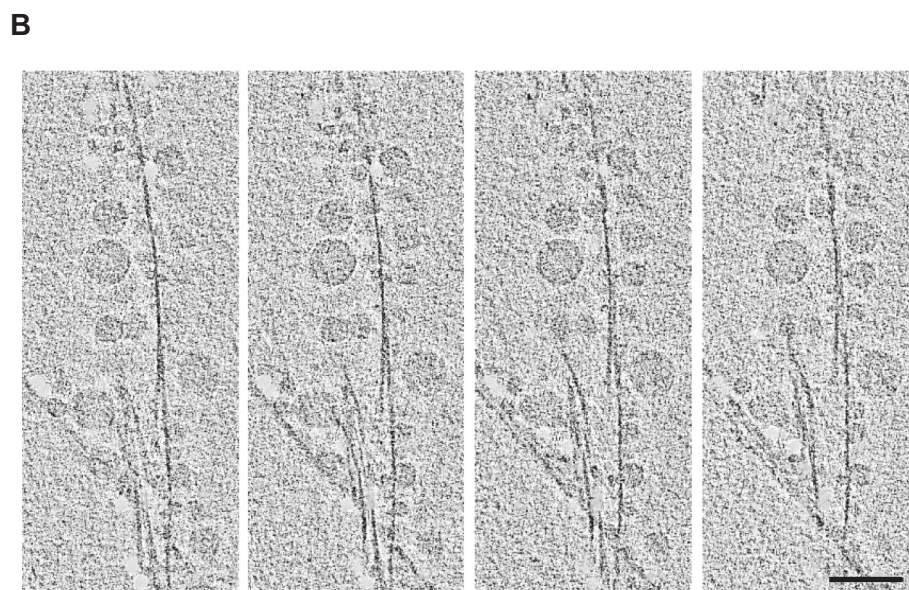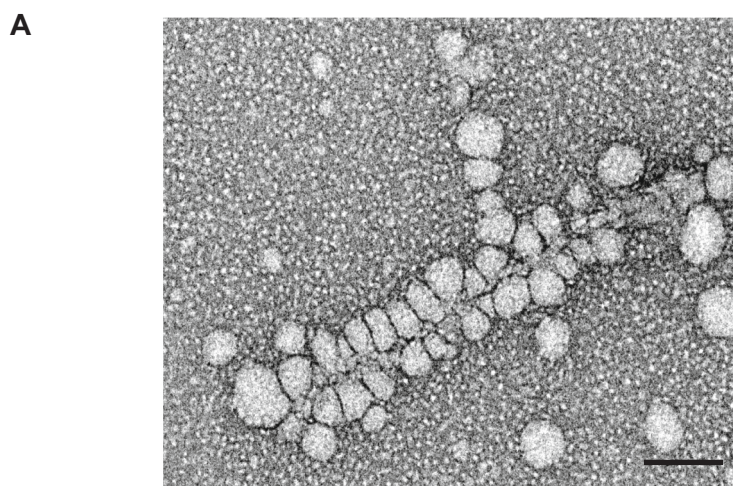
Fig. 2. Observations by cryo-electron microscopy (CEM) and tomography (Cryo-ET) of coupling between the BIOT-NFL-peptide and 50 nm-lipid nanocapsules (LNC). An incubation between 369 μL of 1 mmol/L of peptide and 1 mL of 200 mg/mL of 50 nm-LNC was realized overnight at room temperature under gentle magnetic stirring. (**A**) The BIOT-NFL-peptide coupled with 50 nm-LNC. Observations were performed with a cryo-electron microscope. Micrographs were acquired under low electron doses using the camera in binning mode 1 and at a nominal magnification of 29,000 X. Scale bar: 100 nm, (**B**) Serial and successive slices show that LNCs interact with the nanofilaments formed by the BIOT-NFL-peptide, and this is observed all along the filament in these different planes. Scale bar: 100 nm.

NFL-SCR, or nude-NFL) to obtain a calibration curve for each of these molecules. Then, a mixture of peptide that interacted with the LNCs was injected. We have tested different concentrations of peptide (between 5 and 200 µmol/L) incubated overnight at room temperature under gentle agitation with different concentrations of LNCs (between 5 and 30 mg/mL). With this method, it is impossible to decrease or increase further the concentration of peptide or LNCs otherwise it becomes impossible to assay or it saturates the system. Two peaks were detected: the first corresponding to the LNC-peptide and the second to the free peptide.

For the peptide-LNC mixture, we observed that an increase of the peptide concentration improved the adsorption percentage for the BIOT-NFL, BIOT-NFL-SCR, FAM-NFL, and FAM-NFL-SCR peptides. A mixture of 200 µmol/L of peptide with 30 mg/mL of LNCs gives an adsorption percentage of 95.06 ± 1.19% (Fig. 3A), 84.95 ± 6.61% (Fig. 3B), 86.23 ± 1.32% (Fig. 3C) and 77.32 ± 5.22% (Fig. 3D), for respectively BIOT-NFL, BIOT-NFL-SCR, FAM -NFL, and FAM-NFL-SCR. For the nude-NFL-peptide, the maximum adsorption is obtained with 20 µmol/L of peptide and 30 mg/mL of LNCs (30.61 ± 11.45%; Fig. 3E). The same results were obtained with the both nude-NFL-peptides (data not shown). With LNC concentration at 15 mg/mL, an increase of the adsorption percentage was observed with an increase of the peptide increase (Supplemental Fig. S3A-D) for the BIOT-NFL, BIOT-NFL-SCR, FAM-NFL, and FAM-NFL-SCR-peptides.

To further explore the interaction ability between LNCs and nanofilaments formed by the BIOT-NFL-peptide, we have investigated by cryo-ET the organization of the nanostructures formed between the BIOT-NFL-peptide at 500 µmol/L and the LNC at two concentrations (10 or 30 mg/mL) (Fig. 4). We observed in Fig. 4A, that with a low concentration of LNCs (10 mg/mL), almost the majority of LNCs is located along the filaments formed by the BIOT-NFL-peptide, and very few LNCs are alone and do not interact with the nanofilaments. But with an increased concentration of LNCs (30 mg/mL), many more LNCs are not adsorbed along the nanofilaments and are alone (Fig. 4B). In the paper, we presented the results of the mixture with a concentration of LNCs at 30 mg/mL, and in the supplemental data (Supplemental Fig. S3) we showed the results with a concentration of LNCs at 15 mg/mL. This ultrastructural organization is stable with time (after more than 1 month) and following dilution of LNCs or BIOT-NFL-peptide (data not shown).

3.4. Physicochemical characteristics of LNC-(DiD) alone or functionalized with peptides

To validate the interaction of peptides on LNC surface, three physicochemical characteristics were measured: the mean size, the polydispersity index (PDI), and the zeta potential. Using the Zetasizer, the mean size for respectively LNC-(DiD), LNC-(DiD)-BIOT-NFL, LNC-(DiD)-BIOT-NFL-SCR, LNC-(DiD)-FAM-NFL, LNC-(DiD)-FAM-NFL-SCR, and LNC-(DiD)-nude-NFL was 56.51 ± 2.16 nm, 55.56 ± 2.01 nm, 54.72 ± 0.59 nm, 54.58 ± 5.76 nm, 54.82 ± 1.15 nm, and 64.89 ± 1.56 nm (Table 1). Thus, using this approach, the long filaments formed by the BIOT-NFL-peptide were not detected, nor the long bracelets of LNC-BIOT-NFL, and therefore their length could not be determined. The polydispersity index (PDI) was always less than 0.2, showing that the populations of nanoparticles are homogeneous (Table 1). If the peptide interacts with LNCs, it can be assumed that a change in the zeta potential should be observed. The zeta potential of LNCs is negative (Heurtault et al., 2002), and an interaction with a positive peptide makes the charge of the LNC-peptide less negative. The measures of the zeta potential are negative, -11.36 ± 5.53 mV, -2.55 ± 0.18 mV, -6.11 ± 0.85 mV, -4.41 ± 0.30 mV, -1.58 ± 0.21 mV, and -1.25 ± 0.33 mV for respectively LNC-(DiD), LNC-(DiD)-BIOT-NFL, LNC-(DiD)-BIOT-NFL-SCR, LNC-(DiD)-FAM-NFL, LNC-(DiD)-FAM-NFL-SCR, and LNC-(DiD)-nude-NFL (Table 1). Whatever the nude-NFL used, the results of the mean size, the PDI and the zeta potential are similar. The zeta potential difference between LNC-(DiD) and LNC-(DiD) functionalized with peptides

confirms the peptide interaction with LNC.

3.5. Cellular internalization of LNCs in rat glioblastoma cells is the best with LNC-(DiD)-FAM-NFL

LNC-(DiD) without or with peptides (BIOT-NFL, BIOT-NFL-SCR, FAM-NFL, FAM-NFL-SCR, or nude-NFL) were incubated at different concentrations (0.2, 0.5, 1 or 2 mg/mL of LNC-(DiD)) with F98 cells for 6 h. Then the effect of the different peptides on the internalization of LNC-(DiD) in GBM cells was quantified by flow cytometry. The evaluation of the percentage of DiD in cells showed an increase of fluorescence when the LNC-(DiD) were functionalized with the NFL-peptides (BIOT, FAM, or nude) (Fig. 5A). Internalization was greatest when F98 cells were incubated with LNC-(DiD)-FAM-NFL at 2 mg/mL (22.45 ± 2.80%, 70.02 ± 2.33%, and 17.49 ± 1.67% for respectively LNC-(DiD)-BIOT-NFL, LNC-(DiD)-FAM-NFL, and LNC-(DiD)-nude-NFL) (Fig. 5A). Interestingly, when the LNC-(DiD) were coupled to the BIOT-NFL-SCR-peptide, this did not allow better cell entry, compared to cell internalization when the nanoparticles are functionalized with the BIOT-NFL-peptide (22.45 ± 2.80% and 4.24 ± 0.54% for respectively LNC-(DiD)-BIOT-NFL, and LNC-(DiD)-BIOT-NFL-SCR) (Fig. 5A-B). Similar observations were made when examining the effects of FAM-peptides (70.02 ± 2.33% and 36.26 ± 8.17% for respectively LNC-(DiD)-FAM-NFL, and LNC-(DiD)-FAM-NFL-SCR) (Fig. 5A-B). These experiments showed that the presence of the NFL-peptide (BIOT, FAM, or nu) increases LNC-(DiD) uptake in F98 cells, whereas the SCR-peptides (BIOT, or FAM) has no major effect on LNC cell entry. The best internalization was obtained with LNC-(DiD)-FAM-NFL (Fig. 5).

Finally, confocal microscope analysis was performed using 2 mg/mL of LNC-(DiD) alone or functionalized with different peptides. The concentration chosen is 2 mg/mL to obtain the best visualization of the LNC-(DiD), and confocal observation allows precise localization of the DiD probe and the FAM-coupled peptide. At higher concentrations the observations are saturated by the fluorescence intensity, and at lower concentrations the labeling is not homogeneously detected. In Fig. 6, we observed that the DiD fluorescence in red is higher when F98 cells were treated with LNC-(DiD)-FAM-NFL, and these results confirm measurements realized by flow cytometry (Fig. 5). In general, the DiD fluorescence is greater when the NFL-peptide (BIOT, FAM, or nude) is adsorbed on the surface of LNC-DiD, and when compared to LNC-DiD without peptide. Finally, we can observe in green the presence of Fluorescein bound to the peptide (NFL, or scrambled), and which is generally internalized in F98 cells (Fig. 6).

4. Discussion

Peptide self-assembly represents a promising route to fabricate nanostructures that can be used in the field of nanomedicine and drug targeting (Habibi et al., 2016). The analysis of the BIOT-NFL-peptide by using transmission electron microscopy showed its capacity to spontaneously self-assemble into nanofilaments of about 5 nm in diameter and several micrometers in length (Fig. 1A). Concerning the FAM-NFL-peptide (Fig. 1C), we observed much shorter nanofilaments, and in much smaller quantities. We also investigated the organization of scrambled peptides linked either to Biotin, or Fluorescein. These scrambled peptides have the same amino acids as the NFL-peptide but in a different order, and the electron microscopy showed that such scrambled peptides can self-assemble into nanofilaments, but their ultrastructure is slightly different (Fig. 1B and D). For the nude-NFL-peptide, TEM observations showed the presence of short and rare fibrils (Fig. 1E). This investigation indicates that the formation of filaments by this family of peptides does not concern exclusively the BIOT-NFL-peptide. For additional details, please see the accompanying paper from Alnemeh-Al Ali et al. (Alnemeh-Al Ali et al., 2022).

In Fig. 1A, we have shown that the BIOT-NFL-peptide formed nanofilaments. Two techniques were generally used to visualize
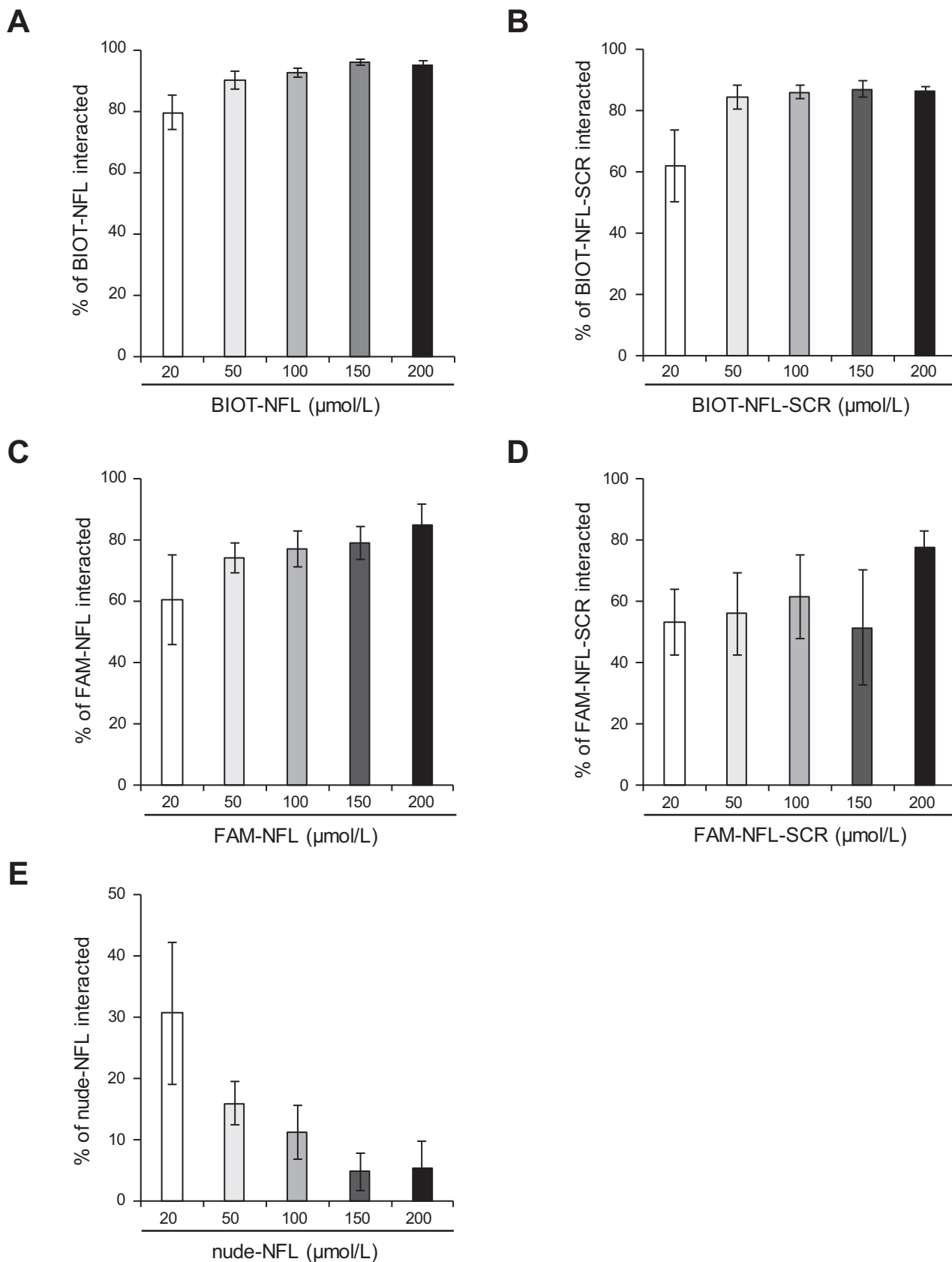
Fig. 3. Quantification of the peptide interaction on the surface of lipid nanocapsules by the Size-Exclusion Chromatography/Ultra-Performance Liquid Chromatography (SEC/UPLC) system. An incubation between 369 µL of peptide and 1 mL of 50 nm-LNC was performed overnight at room temperature under gentle magnetic stirring. The final concentration of 50 nm-LNC are 30 mg/mL, and the concentration of peptide (BIOT-NFL, BIOT-NFL-SCR, FAM-NFL, FAM-NFL-SCR, or nude-NFL) varies between 20 and 200 µmol/L. (**A**) Analysis by UPLC system of percentage of the BIOT-NFL, (**B**) of the BIOT-NFL-SCR, (**C**) of the FAM-NFL, (**D**) of the FAM-NFL-SCR, and (**E**) of the nude-NFL. Experiments were performed at least in triplicate. Data are represented as mean ± SEM.

A

B
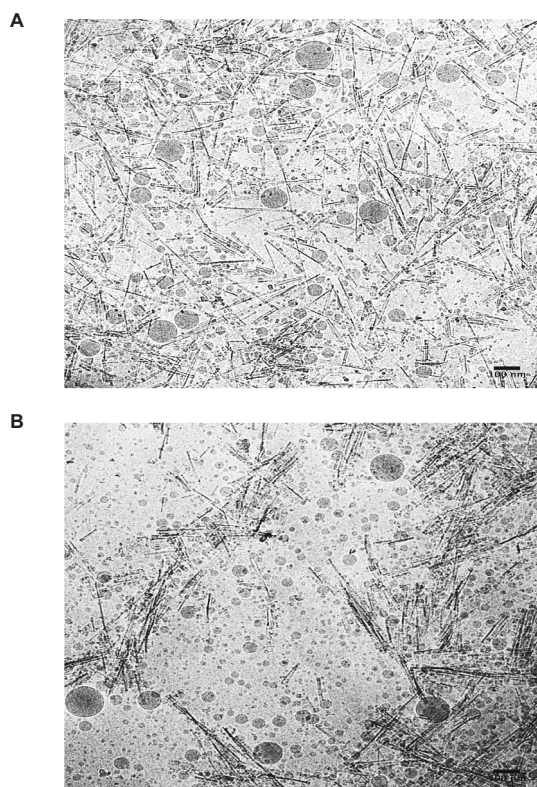
Fig. 4. Observations by cryo-electron microscopy (CEM) of coupling between the BIOT-NFL-peptide and LNC. An incubation between BIOT-NFL-peptide and 50 nm-LNC was realized overnight at room temperature under gentle magnetic stirring. (**A**) Micrographs showing LNC (10 mg/mL), and the BIOT-NFL-peptide (500 μmol/L) were acquired under low electron doses using the camera in binning mode 1. Scale bar: 100 nm. (**B**) Micrographs showing LNC (30 mg/mL), and the BIOT-NFL-peptide (500 μmol/L) were acquired under low electron doses using the camera in binning mode 1. Scale bar: 100 nm.

Table 1

Physicochemical characteristics of 50 nm-LNC-(DiD) alone or functionalized with the BIOT-NFL, the BIOT-NFL-SCR, the FAM-NFL, the FAM-NFL-SCR, or the nude-NFL. An incubation between 369 μL of 1 mmol/L of peptide and 1 mL of 200 mg/mL of 50 nm-LNC-(DiD) was realized overnight at room temperature under gentle magnetic stirring. Three characteristics were measured: the mean size in nanometer (nm), the PDI (polydispersity index), the zeta potential in millivolt (mV), and the conductivity in millisiemens/cm (mS/cm). Experiments were performed at least in triplicate.

Formulations	Size (nm)	PDI	Zeta potential (mV)	Conductivity (mS/cm)
LNC-(DiD)	56.51 +/− 2.16	0.097 +/− 0.026	−11.36 +/− 5.53	0.168 +/− 0.002
LNC-(DiD)-BIOT-NFL	55.56 +/− 2.01	0.125 +/− 0.035	−2.55 +/− 0.18	0.179 +/− 0.007
LNC-(DiD)-BIOT-NFL-SCR	54.72 +/− 0.59	0.162 +/− 0.036	−6.11 +/− 0.85	0.189 +/− 0.004
LNC-(DiD)-FAM-NFL	54.58 +/− 5.76	0.166 +/− 0.010	−4.41 +/− 0.30	0.161 +/− 0.003
LNC-(DiD)-FAM-NFL-SCR	54.82 +/− 1.15	0.121 +/− 0.006	−1.58 +/− 0.21	0.169 +/− 0.003
LNC-(DiD)-nude-NFL	64.89 +/− 1.56	0.119 +/− 0.010	−1.25 +/− 0.33	0.184 +/− 0.007

nanoparticles: cryo-electron microscopy and cryo-electron tomography (Stewart, 2017). These techniques have the advantage of instantly freezing the nano-objects without dehydrating them or using contrasting agents like uranyl acetate. First, by cryo-electron microscopy analysis of the structures formed by the BIOT-NFL-peptide and LNCs, we observed that LNCs were adsorbed along the nanofilaments formed by the BIOT-NFL-peptide. (Fig. 2A). To go further, we performed cryo-electron tomography (cryo-ET) experiments to determine the 3D architecture of the interaction between the filaments formed by the BIOT-NFL-peptide and LNCs. The advantages of using cryo-ET are a better understanding of the three-dimensional organization of nanoparticles composed of lipids and polymers, and a better visualization of the morphology of these nanoparticles (Stewart, 2017). In Fig. 2B, images taken in three successive planes confirmed that LNCs adsorb along the nanofilaments formed by the BIOT-NFL-peptide, and the near absence of free LNC. Moreover, the images showed that LNCs are arranged in a helical fashion along the nanofilaments. Another study showed that gold nanoparticles adsorbed along nanofilaments formed by BIOT-NFL-peptide and this nanosystem can penetrate into F98 GBM cells (Alnemeh-Al Ali et al., 2022). Similarly it was shown that gold nanoparticles adsorbed along filaments formed by C18-(PEPAu^{M-ox})$_2$ peptide (Merg et al., 2016). A much higher magnification and resolution analysis should allow us to understand at the molecular level the importance of the different atoms of each molecule involved in this unique and stable organization. Therefore, these types of electron-cryo-microscopies are extremely useful and essential to study the interaction between LNCs and peptides in monomeric form or in the form of filaments. They allow an extremely fine analysis of their ultrastructural organization.

To use peptide coupled LNCs on GBM models, it is important to define the interaction parameters, such as the amount of peptide adsorbed on LNCs and its stability. For this purpose, we used the Size-Exclusion Chromatography/Ultra-Performance Liquid Chromatography system (SEC/UPLC). This technique was developed by Gazaille et al., and the major difference concerns one of the LNC components: instead of using Span® 80, we used Lipoïd S75–3. In our study, we showed that the different peptides (BIOT-NFL, BIOT-NFL-SCR, FAM-NFL, FAM-NFL-SCR, or nude-NFL) can interact with the LNC (Fig. 3A-E and Supplemental Fig. S3). Our results showed that the difference in LNC composition has no major impact on the detection of LNCs by UPLC. Interestingly, these results show big differences in the ability of different peptides to interact with the same concentration of LNCs, and this difference is not explained by the capacity of peptides to form filaments or not.

An important difference was observed depending on the method used: SEC/UPLC (Fig. 3 and Supplemental Fig. S3) *versus* CEM (Fig. 4). In fact, SEC/UPLC results (Fig. 3A) showed that BIOT-NFL-peptide interact with LNCs, while CEM results indicate saturation when too many LNC are present relative to the amount of peptide (Fig. 4A). When the concentration of LNCs is too high, it is observed that several LNCs do not interact with filaments formed by the BIOT-NFL-peptide (Fig. 4B). Without CEM analysis, we thought that all BIOT-NFL-peptide interacted with LNCs.

The first possible hypothesis to explain this difference may be due to the preparation of the samples. For CEM analysis, the sample fixation is rapid and give structural information, unlike SEC/UPLC analysis samples are not fixed and kept at 4 °C for the duration of the analysis (several hours). Another possible hypothesis may be that during the SEC/UPLC analysis, the interaction between the peptide and LNCs can continue, and so it increases the percentage of peptide-LNC interaction and could explain a saturation observed with certain peptides. These results also indicate that it is necessary to combine several experimental approaches to better understand and characterize the nano-objects formed and their dynamic properties.

With CEM analysis (Fig. 4), we also observed a size heterogeneity of LNCs, heterogeneity not observed with Zetasizer (Table 1). For DLS analysis, the same measurement parameters were used for LNCs and
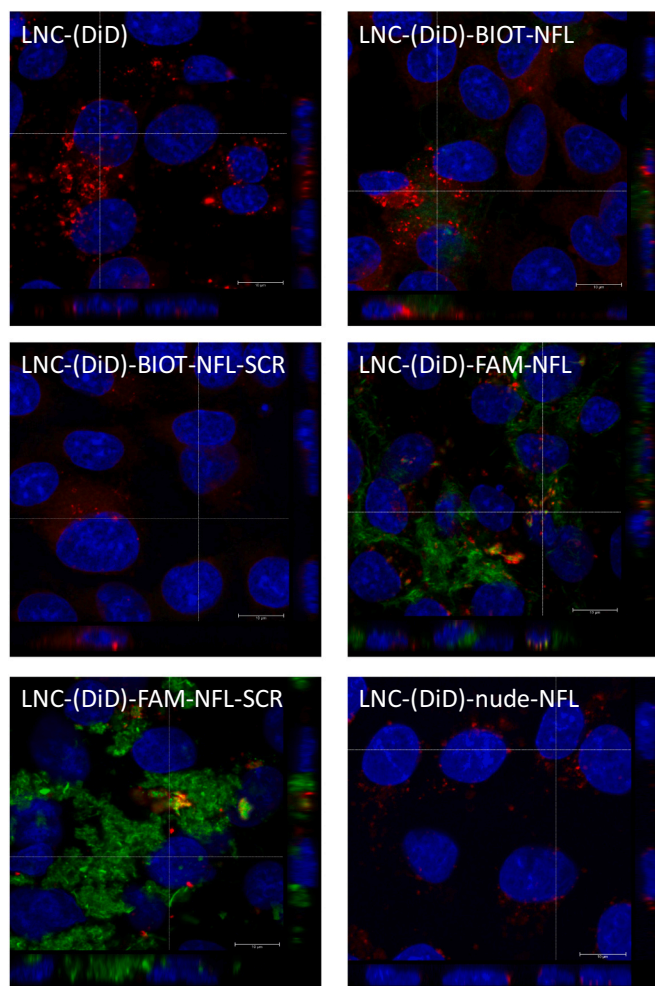
A

B
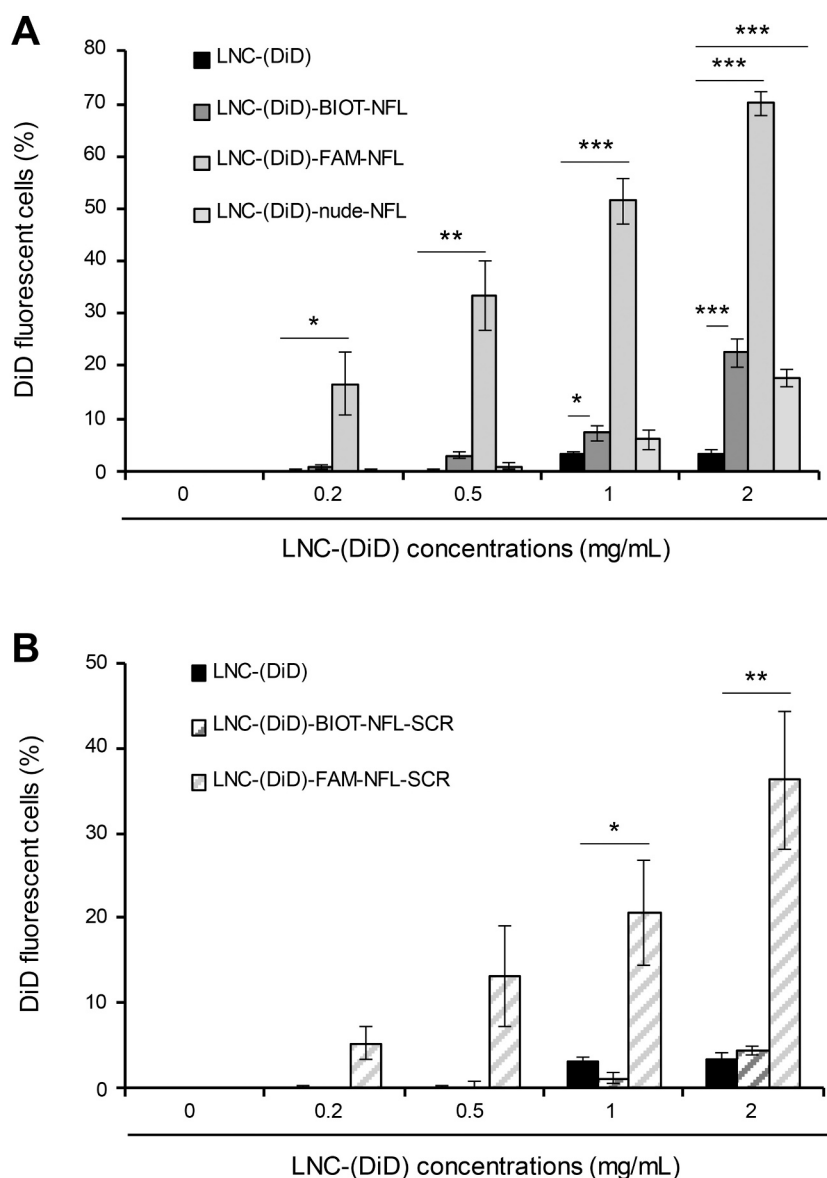
Fig. 5. Cellular uptake of LNC-(DiD) alone or functionalized with the NFL-peptide (BIOT, FAM, or nude) or scrambled peptides (BIOT, or FAM) in F98 cells. Analysis by flow cytometry of F98 cells incubated for 6 h at 37 °C with different concentrations (0.2, 0.5, 1 or 2 mg/mL) of LNC-(DiD) without or with peptides. (**A**) Cells were incubated with LNC-(DiD), LNC-(DiD)-BIOT-NFL, LNC-(DiD)-FAM-NFL, or LNC-(DiD)-nude-NFL; and the DiD fluorescence was measured by flow cytometry. Experiments were performed at least in triplicate, and 20,000 cells were measured for each experiment. Data are represented as mean ± SEM. Statistical analysis was performed with Student's *t*-test (*p < 0.05, **p < 0.005 and ***p < 0.001). (**B**) Cells were incubated with LNC-(DiD), LNC-(DiD)-BIOT-NFL-SCR, and LNC-(DiD)-FAM-NFL-SCR. The fluorescence of the DiD was quantified by flow cytometry. Experiments were performed at least in triplicate, and 20,000 cells were measured for each experiment. Data are represented as mean ± SEM. Statistical analysis was performed with Student's *t*-test (*p < 0.05 and **p < 0.005).

LNC-peptide. And as some peptides can form filaments and adsorb to LNCs, the parameters used may not be able to detect these sort of nano-bracelets. A study showed a difference of size between CEM, and dynamic light scattering (DLS) used by Zetasizer, with nanoparticles smaller with CEM analysis. One explanation for this difference could be the charges of nanoparticles, and if we work at high concentration a charge repulsion can be created. Thus, one advice is to use Tween to prevent agglomeration or aggregation. Another possibility could be to measure the samples in water, which could shift the particle size towards smaller values (Dieckmann et al., 2009). Similar observations regarding the size difference between SEM analysis and DLS analysis have been also described with metal particles (Mahl et al., 2011). In our case, DLS measures indicate principally the size of LNCs and not the size of the filament length formed by BIOT-NFL-peptide, nor the size of the bracelets formed of LNC around nanofilaments.

Lipid nanocapsules functionalized with the NFL-peptide have already been used in several models (Balzeau et al., 2013; Carradori et al., 2020, 2016; Karim et al., 2018), and all the results obtained by different researchers over more than ten years show that the presence of the NFL-peptide on the surface of LNC increases their cellular uptake and their efficiency on GBM cells both *in-vitro* and *in-vivo*. Moreover,

LNCs are biocompatible, escape endosomal lysozyme and may allow delivery of an anti-cancer. Thus, we tested different concentrations of LNC-(DiD) functionalized with the peptides (BIOT-NFL, BIOT-NFL-SCR, FAM-NFL, FAM-NFL-SCR, or nude-NFL) on F98 rat GBM cells. Results obtained by flow cytometry showed that the presence of the NFL-peptide (BIOT, FAM, or nude) increased the cellular uptake of the LNC-(DiD) in F98 cells, and the best cellular uptake was observed when LNC-(DiD) at 2 mg/mL were functionalized with the FAM-NFL-peptide (Fig. 4B). These results were validated by confocal experiments (Fig. 5). We can notice a difference in fluorescence intensity of the DiD probe between flow cytometry experiments (Fig. 4) and those of confocal microscopy (Fig. 5). One hypothesis is cell preparation; indeed, for the flow cytometry we worked on living cells, whereas for the confocal we worked with fixed cells, which could reduce the fluorescence intensity. These relative differences may also be due to the intensities of the laser beams used for flow cytometry or confocal microscopy. Finally, the emission intensity of the two fluorochromes DiD and FAM is different, which could contributes to the obtained differences.

Despite these relative differences and using the complementary information obtained with all these approaches, we consistently found a major interest in using the NFL-peptides (BIOT, FAM, or nude) to

Fig. 6. Confocal experiment to verify the uptake of LNC-(DiD) alone or functionalized with the NFL-peptide (BIOT, FAM, or nude) or scrambled peptides (BIOT, or FAM) in rat GBM cells. F98 cells were incubated 6 h at 37 °C with LNC-(DiD) at 2 mg/mL without or with different peptides (BIOT-NFL, BIOT-NFL-SCR, FAM-NFL, FAM-NFL-SCR, or nude-NFL). Images were taken with a confocal microscope, LNC-(DiD) were visualized in red, the FAM-peptide in green, and nucleus in blue. Experiments were performed at least triplicate. Images were taken with a confocal microscope. Scale bar: 20 μm. (For interpretation of the references to colour in this figure legend, the reader is referred to the web version of this article.)

increase LNC-(DiD) internalization in rat GBM cells. It is important to note that the presence of a special function (Biotin, or Fluorescein) on the NFL-peptide has a good impact on the uptake of LNC-(DiD). Moreover, the cellular internalization is independent of the peptide capacity to form nanofilaments or not. This adsorption could be important because, with the NFL-peptide, better targeting of GBM cells could be achieved by locally concentrating LNCs around the nanofilaments and preventing free LNCs from remaining in the environment.

Other studies have also shown the importance of combining nanoparticles with a targeting peptide. A study has shown that the selectivity and penetration of nanoparticles functionalized with RLW peptide increased the entry of the peptide into spheroids (Gao et al., 2015). Another study showed that gold nanoparticles functionalized with RGD peptide are better internalized in cells than particles alone, and there is also an accumulation of such formulation in the brain and in subcutaneous tumors (Albertini et al., 2019). And finally another study used polymer nanoparticles modified with brain-derived neurotrophic factor peptide and showing increased absorption by neurons (Xu and Chau, 2018). Overall, these results indicate that the functionalization of

nanoparticles with peptides increases their targeting and promotes their cellular internalization in cancer cells. These nano-bracelets could also locally accumulate LNCs that have been bound along the nanofilaments, preventing their off-target effects often present in cancers.

5. Conclusion

This work shows the ability of the BIOT-NFL-peptide to spontaneous assemble and form a lot of nanofilaments. Lipid nanocapsules (LNC) adsorb on these nanofilaments, forming together nano-bracelets. Although not all NFL derived peptides form nanofilaments, they are all capable of adsorbing to LNC. The FAM-NFL-peptide form rare nanofilaments, but when it is incubated with LNC-(DiD), the cellular internalization in GBM cells is greater than that obtained with LNC-(DiD)-BIOT-NFL. Filament formation is not essential for proper cellular internalization of LNCs but could prevent their off-target effects.

Declaration of Competing Interest

The authors declare that to the best of their knowledge they have no conflict of interest, with respect to the research, authorship, and/or publication of this article.

Appendix A. Supplementary data

Supplementary data to this article can be found online at https://doi.org/10.1016/j.ijpx.2022.100127.

References

Albertini, B., Mathieu, V., Iraci, N., Van Woensel, M., Schoubben, A., Donnadio, A., Greco, S.M.L., Ricci, M., Temperini, A., Blasi, P., Wauthoz, N., 2019. Tumor targeting by peptide-decorated gold nanoparticles. Mol. Pharm. 16, 2430–2444. https://doi.org/10.1021/acs.molpharmaceut.9b00047.

Alnemeh-Al Ali, H., Griveau, A., Artzner, F., Dupont, A., Lautram, N., Jourdain, M.-A., Eyer, J., 2022. Investigation on the Self-Assembly of the NFL-TBS.40-63 Peptide and its Interaction with Gold Nanoparticles as a Delivery Agent for Glioblastoma submitted.

Balzeau, J., Pinier, M., Berges, R., Saulnier, P., Benoit, J.P., Eyer, J., 2013. The effect of functionalizing lipid nanocapsules with NFL-TBS.40-63 peptide on their uptake by glioblastoma cells. Biomaterials 34, 3381–3389. https://doi.org/10.1016/j.biomaterials.2013.01.068.

Barry, J.N., Vertegel, A.A., 2013. Nanomaterials for protein-mediated therapy and delivery. Nano Life 03, 1343001. https://doi.org/10.1142/S1793984413430010.

Berges, R., Balzeau, J., Peterson, A.C., Eyer, J., 2012. A tubulin binding peptide targets glioma cells disrupting their microtubules, blocking migration, and inducing apoptosis. Mol. Ther. 20, 1367–1377. https://doi.org/10.1038/mt.2012.45.

Carradori, D., Saulnier, P., Préat, V., Des Rieux, A., Eyer, J., 2016. NFL-lipid nanocapsules for brain neural stem cell targeting in vitro and in vivo. J. Control. Release 238, 253–262. https://doi.org/10.1016/j.jconrel.2016.08.006.

Carradori, D., Labrak, Y., Miron, V.E., Saulnier, P., Eyer, J., Préat, V., Des Rieux, A., 2020. Retinoic acid-loaded NFL-lipid nanocapsules promote oligodendrogenesis in focal white matter lesion. Biomaterials 230, 119653. https://doi.org/10.1016/j.biomaterials.2019.119653.

Dieckmann, Y., Cölfen, H., Hofmann, H., Petri-Fink, A., 2009. Particle size distribution measurements of manganese-doped ZnS nanoparticles. Anal. Chem. 81, 3889–3895. https://doi.org/10.1021/ac900043y.

Dubochet, J., McDowall, A.W., 1981. Vitrification of pure water for electron microscopy. J. Microsc. 124, 3–4. https://doi.org/10.1111/j.1365-2818.1981.tb02483.x.

Duchesne, L., Gentili, D., Comes-Franchini, M., Fernig, D.G., 2008. Robust ligand shells for biological applications of gold nanoparticles. Langmuir 24, 13572–13580. https://doi.org/10.1021/la802876u.

Gao, H., Zhang, S., Cao, S., Yang, Y., Pang, Z., Jiang, X., 2014. Angiopep-2 and activatable cell-penetrating peptide dual-functionalized nanoparticles for systemic glioma-targeting delivery. Mol. Pharm. 11, 2755–2763. https://doi.org/10.1021/mp500113p.

Gao, H., Zhang, Q., Yang, Y., Jiang, X., He, Q., 2015. Tumor homing cell penetrating peptide decorated nanoparticles used for enhancing tumor targeting delivery and therapy. Int. J. Pharm. 478, 240–250. https://doi.org/10.1016/j.ijpharm.2014.11.029.

Gazaille, C., Sicot, M., Akiki, M., Lautram, N., Dupont, A., Saulnier, P., Eyer, J., Bastiat, G., 2021. Characterization of biological material adsorption to the surface of nanoparticles without a prior separation step: a case study of glioblastoma-targeting peptide and lipid nanocapsules. Pharm. Res. 38, 681–691. https://doi.org/10.1007/s11095-021-03034-8.

Guyon, L., Lepeltier, E., Gimel, J.-C., Calvignac, B., Franconi, F., Lautram, N., Dupont, A., Bourgaux, C., Pigeon, P., Saulnier, P., Jaouen, G., Passirani, C., 2019. Importance of combining advanced particle size analysis techniques to characterize cell-penetrating peptide–ferrocifen self-assemblies. J. Phys. Chem. Lett. 10, 6613–6620. https://doi.org/10.1021/acs.jpclett.9b01493.

Habibi, N., Kamaly, N., Memic, A., Shafiee, H., 2016. Self-assembled peptide-based nanostructures: smart nanomaterials toward targeted drug delivery. Nano Today 11, 41–60. https://doi.org/10.1016/j.nantod.2016.02.004.

Heurtault, B., Saulnier, P., Pech, B., Proust, J.E., Benoit, J.P., 2002. A novel phase inversion-based process for the preparation of lipid nanocarriers. Pharm. Res. 19, 875–880. https://doi.org/10.1023/A:1016121319668.

Heurtault, B., Saulnier, P., Pech, B., Venier-Julienne, M.-C., Proust, J.-E., Phan-Tan-Luu, R., Benoît, J.-P., 2003. The influence of lipid nanocapsule composition on their size distribution. Eur. J. Pharm. Sci. 18, 55–61. https://doi.org/10.1016/s0928-0987(02)00241-5.

Jiang, T., Zhang, Z., Zhang, Y., Lv, H., Zhou, J., Li, C., Hou, L., Zhang, Q., 2012. Dual-functional liposomes based on pH-responsive cell-penetrating peptide and hyaluronic acid for tumor-targeted anticancer drug delivery. Biomaterials 33, 9246–9258. https://doi.org/10.1016/j.biomaterials.2012.09.027.

Karim, R., Lepeltier, E., Esnault, L., Pigeon, P., Lemaire, L., Lepinoux-Chambaud, C., Clere, N., Jaouen, G., Eyer, J., Piel, G., Passirani, C., 2018. Enhanced and preferential internalization of lipid nanocapsules into human glioblastoma cells: effect of a surface-functionalizing NFL peptide. Nanoscale 10, 13485–13501. https://doi.org/10.1039/c8nr02132e.

Kreuter, J., 2004. Influence of the surface properties on nanoparticle-mediated transport of drugs to the brain. J. Nanosci. Nanotechnol. 4, 484–488. https://doi.org/10.1166/jnn.2003.077.

Lazăr, L.F., Olteanu, E.D., Iuga, R., Burz, C., Achim, M., Clichici, S., Tefas, L.R., Nenu, I., Tudor, D., Baldea, I., Filip, G.A., 2019. Solid lipid nanoparticles: vital characteristics and prospective applications in cancer treatment. Crit. Rev. Ther. Drug Carr. Syst. 36, 537–581. https://doi.org/10.1615/CritRevTherDrugCarrierSyst.2019020396.

Mahl, D., Diendorf, J., Meyer-Zaika, W., Epple, M., 2011. Possibilities and limitations of different analytical methods for the size determination of a bimodal dispersion of metallic nanoparticles. Colloid Surf. A Physicochem. Eng. Asp. 377, 386–392. https://doi.org/10.1016/j.colsurfa.2011.01.031.

Malmsten, M., Lindman, B., 1992. Self-assembly in aqueous block copolymer solutions. Macromolecules 25, 5440–5445. https://doi.org/10.1021/ma00046a049.

Mastronarde, D.N., 1997. Dual-axis tomography: an approach with alignment methods that preserve resolution. J. Struct. Biol. 120, 343–352. https://doi.org/10.1006/jsbi.1997.3919.

Merg, A.D., Boatz, J.C., Mandal, A., Zhao, G., Mokashi-Punekar, S., Liu, C., Wang, X., Zhang, P., van der Wel, P.C.A., Rosi, N.L., 2016. Peptide-directed assembly of single-helical gold nanoparticle superstructures exhibiting intense chiroptical activity. J. Am. Chem. Soc. 138, 13655–13663. https://doi.org/10.1021/jacs.6b07322.

Pudlarz, A., Szemraj, J., 2018. Nanoparticles as carriers of proteins, peptides and other therapeutic molecules. Open Life Sci. 13, 285–298. https://doi.org/10.1515/biol-2018-0035.

Qin, Y., Zhang, Q., Chen, H., Yuan, W., Kuai, R., Xie, F., Zhang, L., Wang, X., Zhang, Z., Liu, J., He, Q., 2012. Comparison of four different peptides to enhance accumulation of liposomes into the brain. J. Drug Target. 20, 235–245. https://doi.org/10.3109/1061186X.2011.639022.

Rudolph, C., Schillinger, U., Ortiz, A., Tabatt, K., Plank, C., Müller, R.H., Rosenecker, J., 2004. Application of novel solid lipid nanoparticle (SLN)-gene vector formulations based on a dimeric HIV-1 TAT-peptide in vitro and in vivo. Pharm. Res. 21, 1662–1669. https://doi.org/10.1023/B:PHAM.0000041463.56768.ec.

Schnyder, A., Krähenbühl, S., Drewe, J., Huwyler, J., 2005. Targeting of daunomycin using biotinylated immunoliposomes: Pharmacokinetics, tissue distribution and in vitro pharmacological effects. J. Drug Target. 13, 325–335. https://doi.org/10.1080/10611860500206674.

Schwarze, S.R., 1999. In vivo protein transduction: delivery of a biologically active protein into the mouse. Science 285, 1569–1572. https://doi.org/10.1126/science.285.5433.1569.

Shapira, A., Livney, Y.D., Broxterman, H.J., Assaraf, Y.G., 2011. Nanomedicine for targeted cancer therapy: towards the overcoming of drug resistance. Drug Resist. Updat. 14, 150–163. https://doi.org/10.1016/j.drup.2011.01.003.

Stewart, P.L., 2017. Cryo-electron microscopy and cryo-electron tomography of nanoparticles. Wiley Interdiscip. Rev. Nanomed. Nanobiotechnol. 9, e1417 https://doi.org/10.1002/wnan.1417.

Suri, S., Fenniri, H., Singh, B., 2007. Nanotechnology-based drug delivery systems. J. Occup. Med. Toxicol. 2, 16. https://doi.org/10.1186/1745-6673-2-16.

Vivès, E., Brodin, P., Lebleu, B., 1997. A truncated HIV-1 Tat protein basic domain rapidly translocates through the plasma membrane and accumulates in the cell nucleus. J. Biol. Chem. 272 (25), 16010–16017. https://doi.org/10.1074/jbc.272.25.16010, 1997 Jun 20.

Wei, W., Wang, Y., Huang, X., Hou, H., Zhou, S., 2018. Peptide-based nanocarriers for cancer therapy. Small Methods 2, 1700358. https://doi.org/10.1002/smtd.201700358.

Xin, H., Jiang, X., Gu, J., Sha, X., Chen, L., Law, K., Chen, Y., Wang, X., Jiang, Y., Fang, X., 2011. Angiopep-conjugated poly(ethylene glycol)-co-poly(ε-caprolactone) nanoparticles as dual-targeting drug delivery system for brain glioma. Biomaterials 32, 4293–4305. https://doi.org/10.1016/j.biomaterials.2011.02.044.

Xu, J., Chau, Y., 2018. Polymeric nanoparticles decorated with BDNF-derived peptide for neuron-targeted delivery of PTEN inhibitor. Eur. J. Pharm. Sci. 124, 37–45. https://doi.org/10.1016/j.ejps.2018.08.020.

Zhu, L., Zhou, Z., Mao, H., Yang, L., 2017. Magnetic nanoparticles for precision oncology: theranostic magnetic iron oxide nanoparticles for image-guided and targeted cancer therapy. Nanomedicine 12, 73–87. https://doi.org/10.2217/nnm-2016-0316.